

In situ generation of plasmonic cavities for high sensitivity fluorophore and biomolecule detection

Daragh Byrne^{1*}, Colette McDonagh¹

¹ School of Physical Sciences, Dublin City University, Glasnevin, Dublin 9, Ireland

*Corresponding Author: Daragh.byrne2@mail.dcu.ie

Supplementary Information

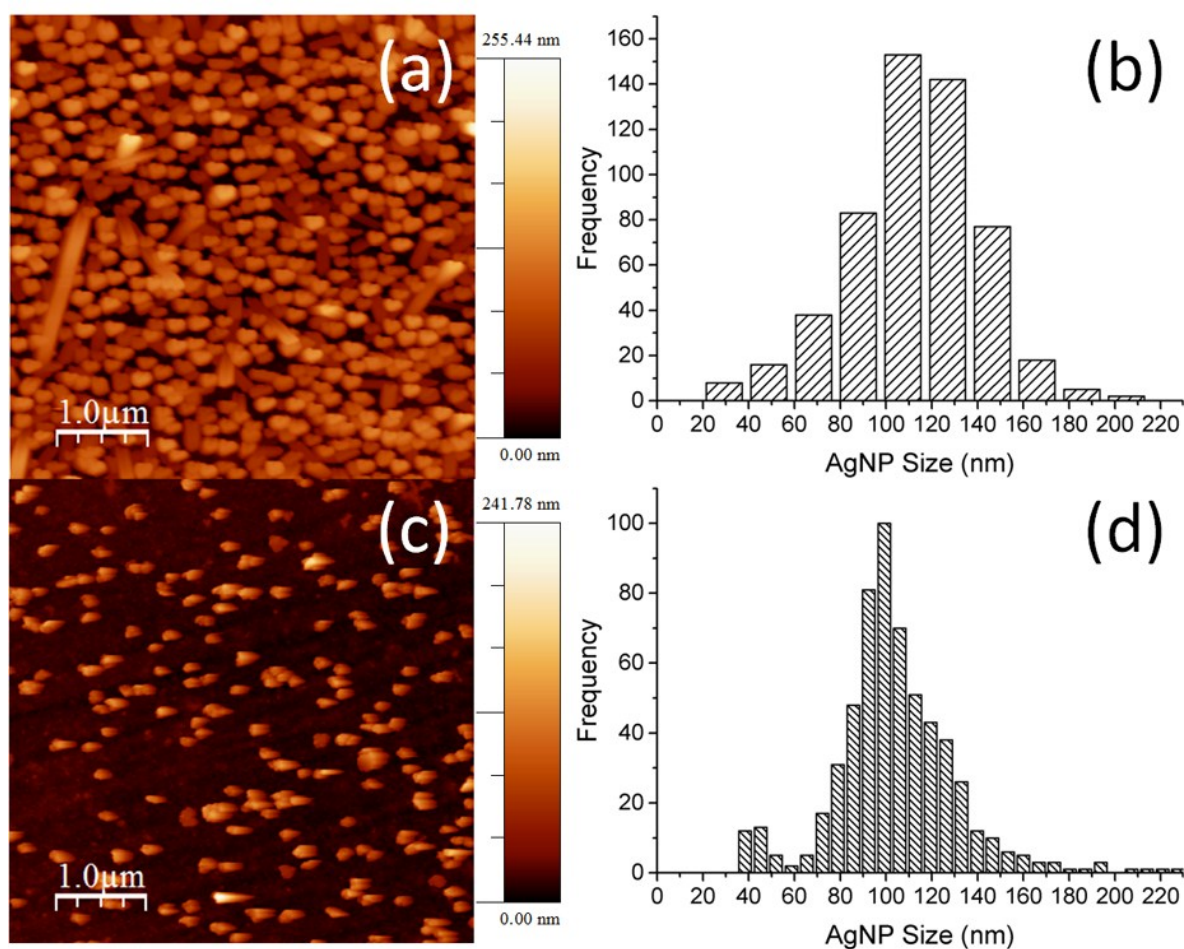


Figure S1 (a) AFM image of solution grown AgNP and (b) corresponding AgNP size distribution. (c) AFM image of *in situ* grown AgNP and (d) corresponding AgNP size distribution.

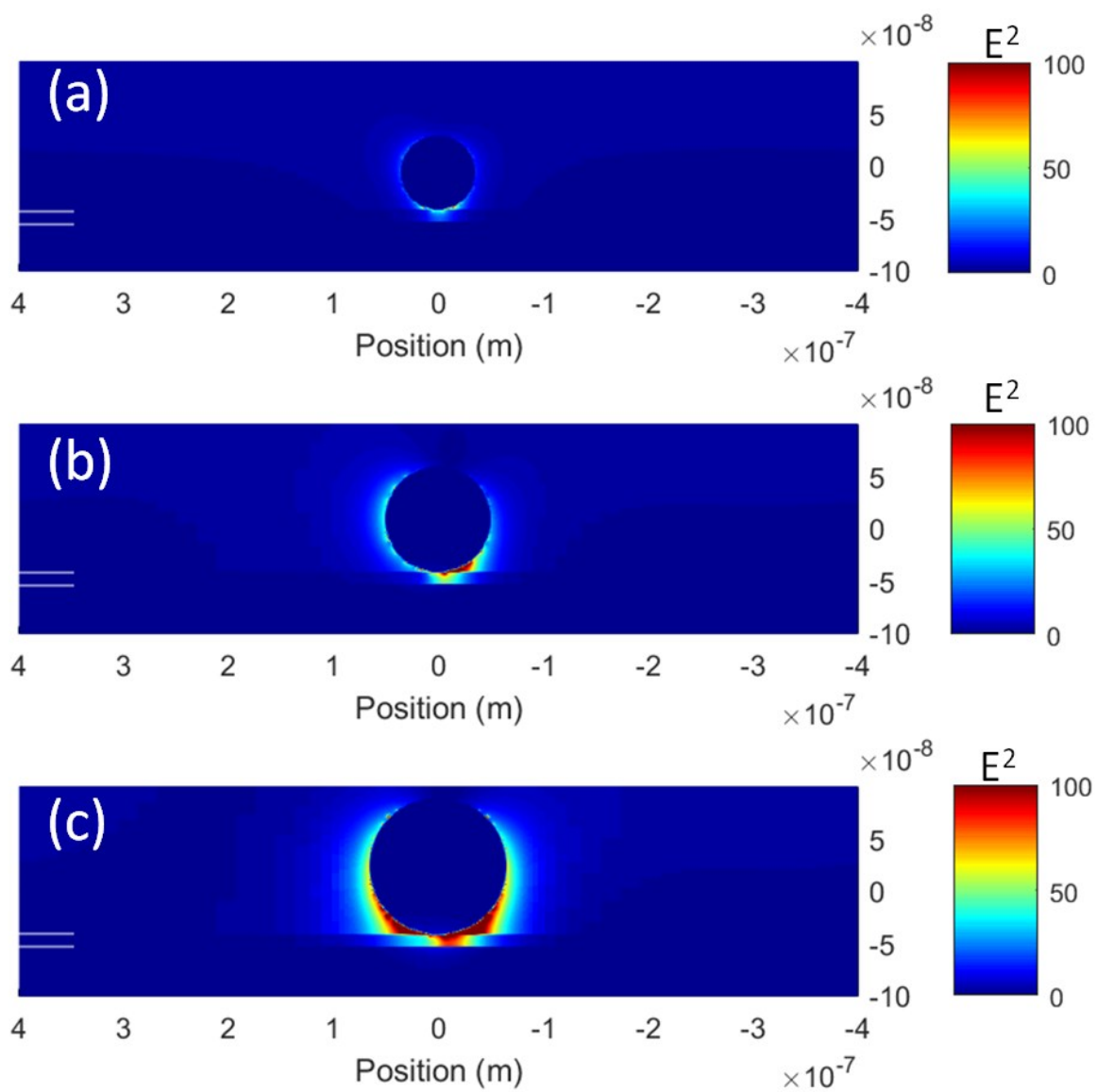


Figure S2: Electric field intensity for (a) Au - 70 nm AgNP Cavity (b) Au - 100 nm AgNP Cavity (c) Au - 130 nm AgNP Cavity. The polyelectrolyte film position is indicated by the white lines.

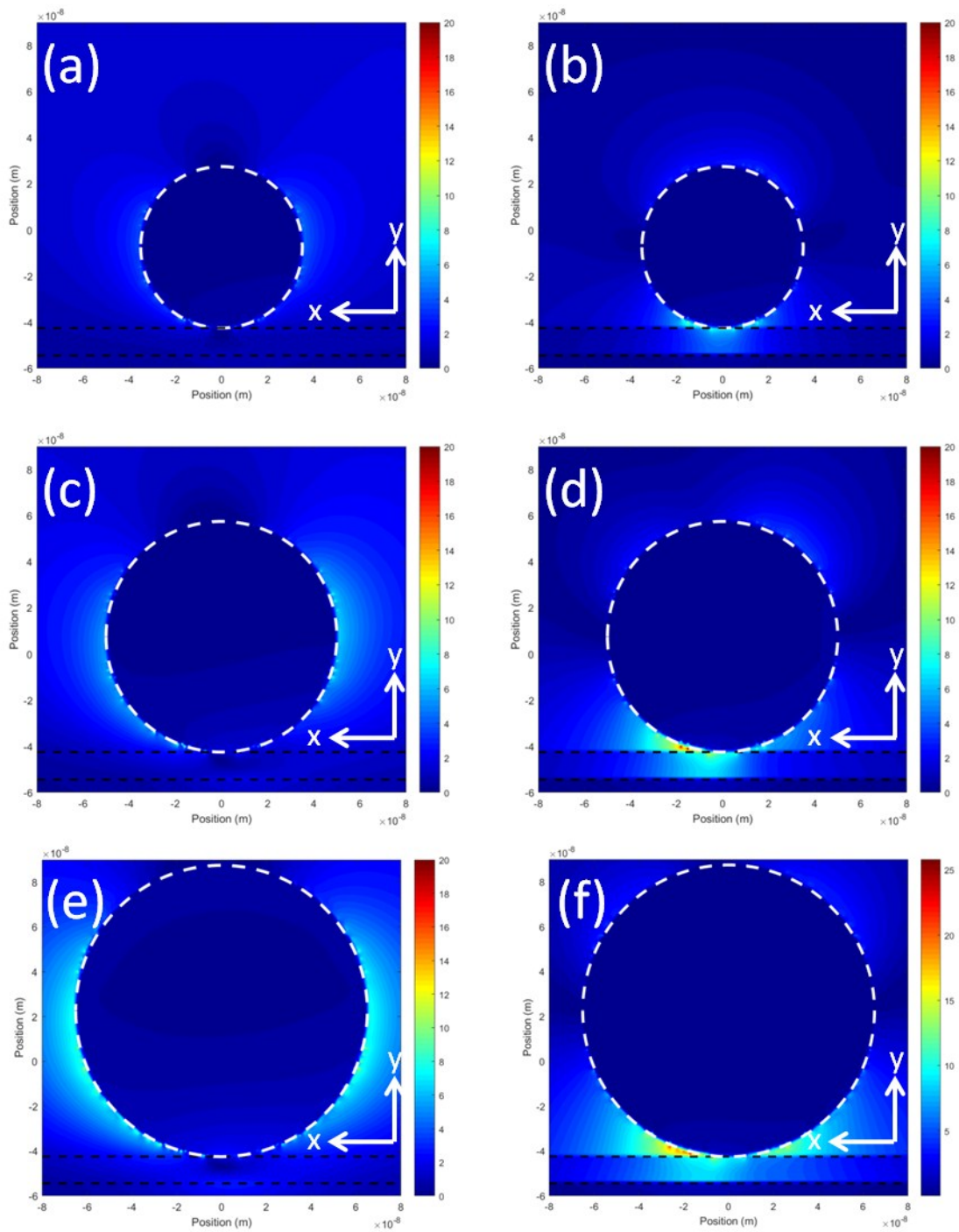


Figure S3: Electric field components for the range of Au-AgNP cavity sizes (a)Ex 70nm AgNP (b) Ey 70nm AgNP (c) Ex 100 nm AgNP (d) Ey 100 nm AgNP (e) Ex 130 nm AgNP (f) Ey 130 nm AgNP. Dashed white line indicated AgNP position. Dashed Black line indicated polyelectrolyte film position.

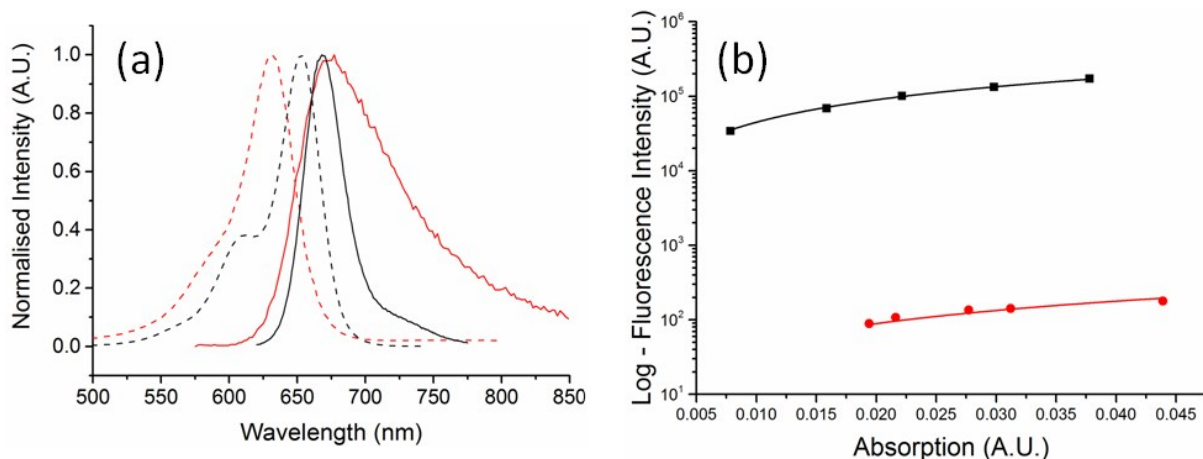


Figure S4: (a) Optical properties of high q^0 and low q^0 dyes. Solid black line: Normalized fluorescence spectrum of Alexa Fluor 647. Dashed black line: Normalized absorption spectrum of Alexa Fluor 647. Solid red line: Normalized fluorescence spectrum of Erioglaucine. Dashed red line: Normalized absorption spectrum of Erioglaucine. (b) Plot of Fluorescence intensity versus absorption for: black squares Alexa Fluor 647. Black line: linear fit of Alexa Fluor 647 data. Red squares: Erioglaucine. Red line: linear fit of Erioglaucine data.

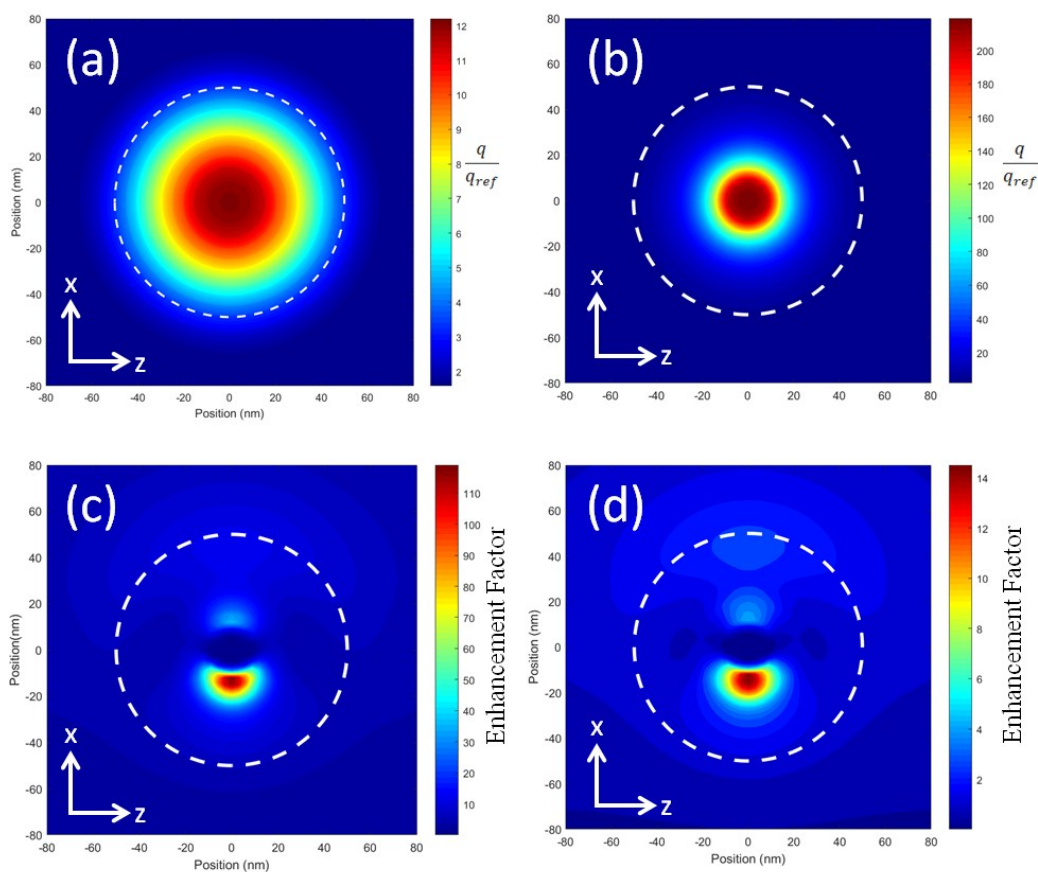


Figure S5: $\frac{q}{q_{ref}}$ Ratio for (a) Alexa Fluor 647 and (b) Erioglaucine fluorophore embedded within the polyelectrolyte layer. (c) Enhancement factor for Ex orientated Alexa Fluor 647 dipole moment. (d) Enhancement factor for Ex orientated Erioglaucine dipole moment. Dashed white line indicates AgNP position.

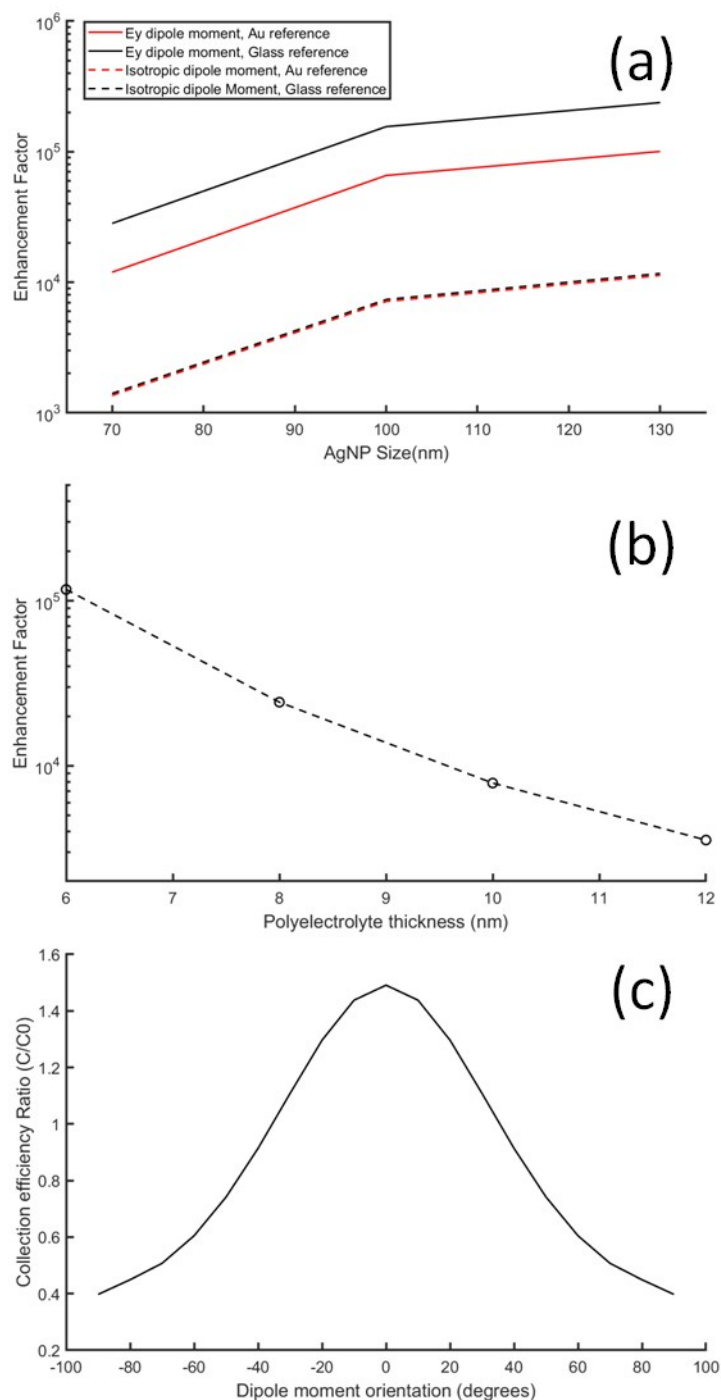


Figure S6: Enhancement factor for Erioglucine at a single point directly beneath an AgNP at the polyelectrolyte centre as a function of (a) AgNP size (b) polyelectrolyte thickness. (c) Ratio of the simulated collection efficiencies for a system with a numerical aperture of 0.5. for a fluorophore under an AgNP (C) versus a fluorophore on a plain Au Film (C0) as a function of the dipole moment angle. An angle of 0° corresponds to a dipole perfectly aligned along E_y . In each case the collected power was normalized to the actual emitted dipole power to compensate for the system's Purcell enhancement.

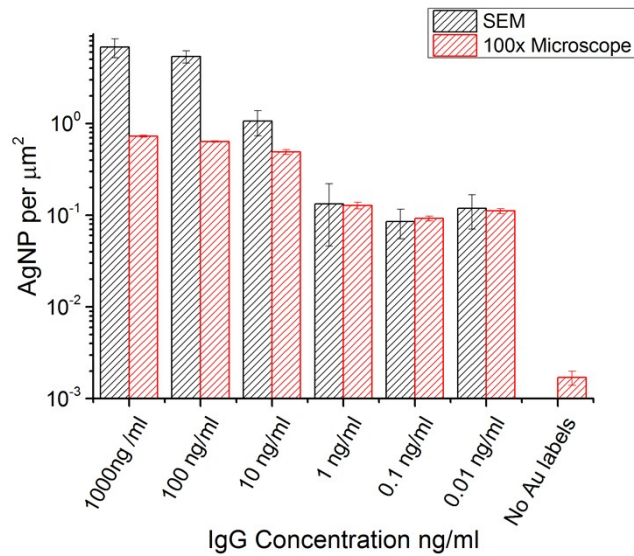


Figure S7: AgNP densities measured from both SEM images and fluorescent microscopy images.

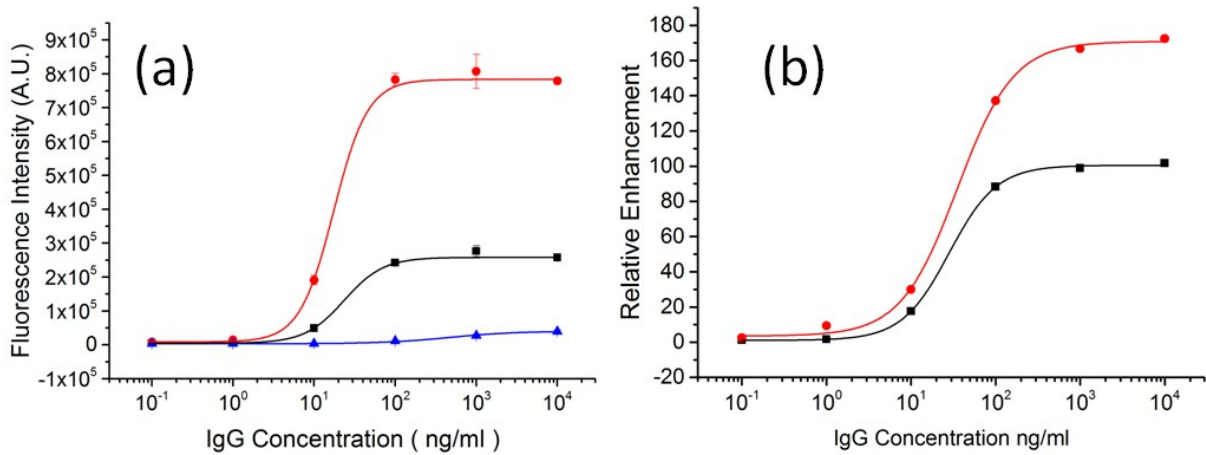


Figure S8: (a) Calibration curve for a IgG assay. Assay performed on Au / PE coated substrate with blue line: Alexa Fluor 647 fluorophore, black line: Erioglaucine in conjunction with *in situ* AgNP growth, red line: *in situ* AgNP post application of 50 μl of Erioglaucine solution for 10 minutes and subsequently washed with DI- H_2O . (b) Relative enhancement of the AgNP ensemble with respect to 0 ng/ml control. Black line: *in situ* AgNP Red line: *in situ* AgNP post additional dye application. All data point in both a and b were fitted using a 4 parameter logistic fit.

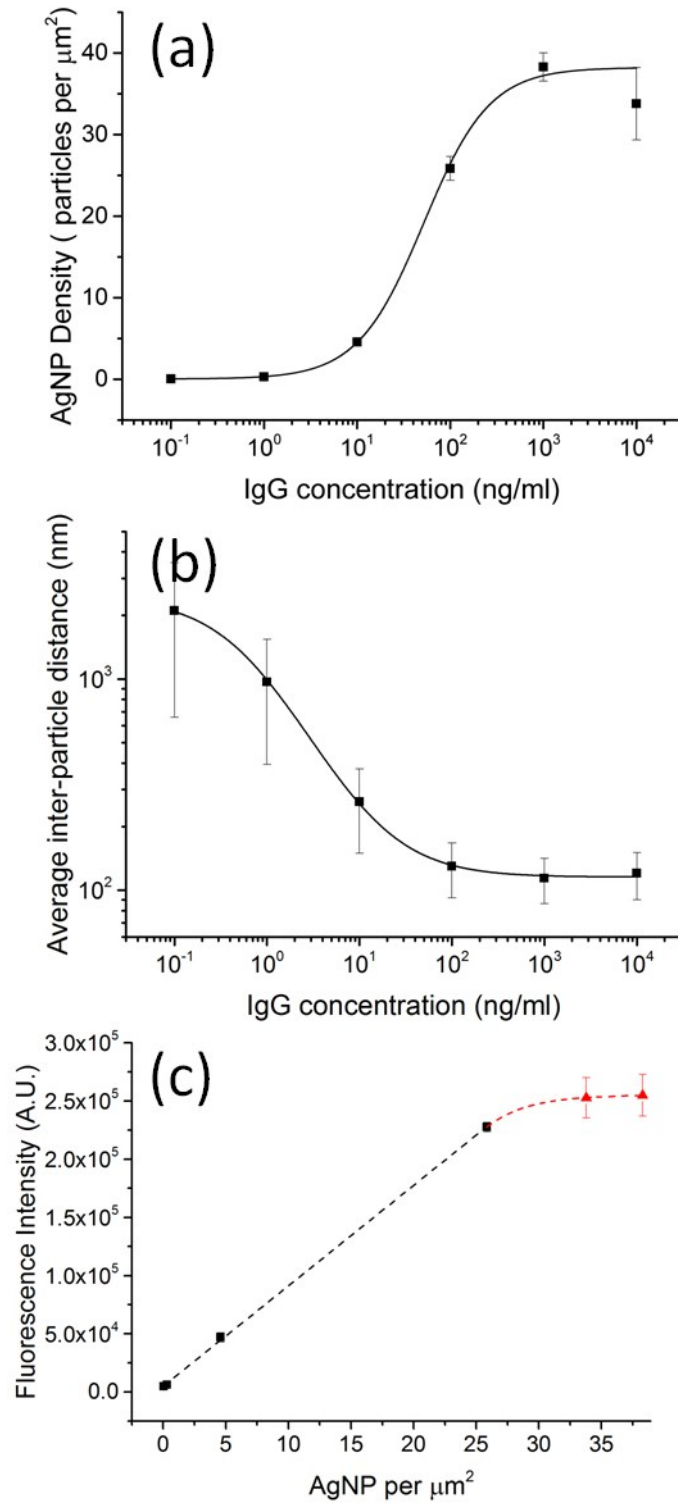


Figure S9: (a) *In situ* grown AgNP density versus IgG concentration. (b) Average inter-particle distance between the centre points of AgNPs. (c) Fluorescence intensity from the *in situ* grown AgNP. Black dashed line: Linear fit of data points Red dashed line: Non-linear fit of data points.

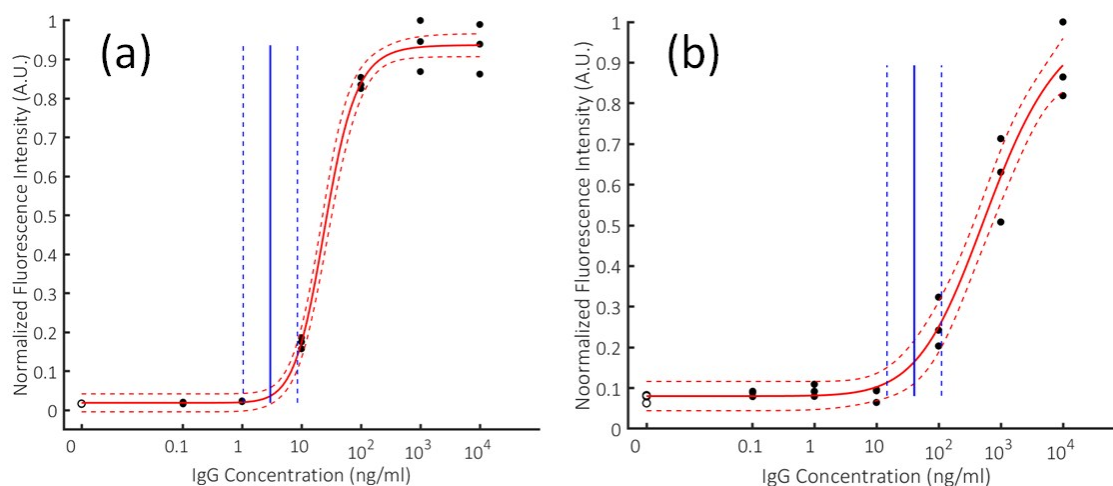


Figure S10: Fit of the calibration curve for (a) in situ grown AgNP and (b) AF-647 labeled antigens. Black solid circles: Assay data points. Black open circles: 0 ng/ml controls. Red solid lines: Four parameter logistic fit of data points. Red dashed lines: Four parameter logistic fit of the data 95% confidence intervals. Blue solid lines: Limits of detection. Blue dashed line: 95% confidence interval of the limits of detection.

Limit of detection analysis

A common approach to determining the analytical sensitivity is to use a zero concentration control plus 3σ to describe the lowest concentration which can be distinguished from zero. This idealized approach neglects the variation observed within the range of non-zero concentrations and may lead to type two errors.¹ In the method proposed here, the quantification of antigens is performed from the amplification of a fluorescent substrate through the formation of cavities and not from the direct binding of fluorophores. This additional step requires more care to ensure that the values at low analyte concentrations are valid as the loss of fluorophores during processing can lead to an artificially low background signal. To address this potential limitation we use the more rigorous approach of Holstein *et al* which incorporates a pooled signal standard deviation to better reflect the variation observed across the sample set and prevent type two errors. The standard deviation of the signal is strongly correlated with the concentration of analyte. Therefore the pooled standard deviation was calculated from the lowest five concentrations (0 ng/ml – 10^2 ng/ml). An identical range was taken for both the AB-9 and AF-647 calibration curves. Figure S10 show the fitted four parameter logistic functions along with the 95% confidence intervals and LODs for both the AB-9 and AF-647 calibration curves. Full details of the calculation procedure and matlab code are provided in reference 1.

References

1. Holstein, C. A.; Griffin, M.; Hong, J.; Sampson, P. D., Statistical Method for Determining and Comparing Limits of Detection of Bioassays. *Analytical Chemistry* **2015**, *87* (19), 9795-9801.